RSC Advances

PAPER

View Article Online
View Journal | View Issue

Cite this: *RSC Adv.*, 2015, **5**, 71709

Antibacterial activities of polymeric poly(DL-lactide-*co*-glycolide) nanoparticles and Soluplus® micelles against *Staphylococcus epidermidis* biofilm and their characterization†

Chisato Takahashi, Shoko Saito, Asami Suda, Noriko Ogawa, Yoshiaki Kawashima and Hiromitsu Yamamoto*

Received 15th July 2015
Accepted 30th July 2015

DOI: 10.1039/c5ra13885j

www.rsc.org/advances

Preparation method of polymeric micelles based on polyvinyl caprolactam–polyvinyl acetate–polyethylene glycol graft copolymer (Soluplus®) have been successfully established as nanocarriers for a drug delivery system on a biofilm formed by *Staphylococcus epidermidis*. The biodegradable poly(DL-lactide-*co*-glycolide) (PLGA) nanoparticles were also prepared for comparison. To design effective nanocarriers against biofilm infections, we tested the four types of polymeric nanocarriers on the biofilm: unmodified PLGA, PLGA modified with chitosan (CS), unmodified Soluplus® micelles (Sol), and Sol modified with CS. The antibacterial activity of each nanocarrier against the biofilm was evaluated using field emission scanning electron microscopy (FE-SEM) with hydrophilic ionic liquid (IL) and confocal laser scanning microscopy. FE-SEM results revealed the exact morphology of carriers and bacterial cells at the nanoscale level by an optimized method using IL. The nanocarriers adhering to the biofilm were quantified using the phenol–sulfuric acid method. Antibacterial activity of nanocarriers was determined by minimum inhibitory concentration and minimum bactericidal concentration, and antibacterial assay using LIVE/DEAD BacLight bacterial viability kit. The highest antibacterial activity against the biofilm was demonstrated by a prepared Sol modified with CS. This nanocarrier would be useful for curing biofilm infections. In addition, visualization of the antibacterial activity at the nanoscale level could help in designing effective nanocarriers for target agents.

Introduction

In recent years, the medical field has achieved remarkable development in advanced medical technology. With this medical progress, implanted medical devices, such as catheters, pacemakers, prosthetic joints, and intraocular lenses, are routinely used in patients.[1,2] However, these devices often cause infections due to bacterial adsorption and growth with biofilm formation on their surface.[3–5] The biofilm promotes the persistence of pathogens in the host, leading to refractory infections, such as periodontal diseases, nosocomial infectious diseases, and osteomyelitis.[6–8] A biofilm consists of bacterial cells covered by a thick film of extracellular polymeric substance (EPS) matrix.[9,10] Once a biofilm is formed, it is difficult to remove it from the substrate using antibacterial drugs. To overcome these infections, we focused on a drug delivery system (DDS) using nanocarriers. Polymeric nanosized carriers possess the following advantageous properties: controlled release, high stability, and enhanced absorption of drugs.[11,12] In our previous studies, we demonstrated the advantages of submicron-sized biodegradable poly(DL-lactide-*co*-glycolide) (PLGA) nanoparticles (NPs) in cancer, gene delivery, and chemotherapy of brain tumors.[13–18] Recently, a new type of polymer, polyvinyl caprolactam–polyvinyl acetate–polyethylene glycol graft copolymer (Soluplus®), was approved for marketing. Soluplus® is a novel amphiphilic polymer applicable for poorly soluble drugs because these drugs can be trapped inside micelles. Other techniques for improving the water solubility of drugs include extrusion techniques, solvent evaporation, and spray-drying techniques.[19–21] In the present study, we targeted the development nano drug carriers with Soluplus® for treatment of biofilm infection disease. There is no report that nanocarriers based on Soluplus® provide high antibacterial activity to microorganism under biofilm. It is believed that nanocarriers around 50 to 350 nm in size exert antibacterial effects according to their sizes.

Generally, quantitative analyses and macroscopic observations were performed for designing polymeric nanocarriers for DDS. However, the morphology and structure of nanocarriers

Pharmaceutical Engineering, School of Pharmacy, Aichi Gakuin University, 1-100, Kusumoto-cho, Chikusa-ku, Nagoya, Aichi 464-8650, Japan. E-mail: hiromitu@dpc.agu.ac.jp; Fax: +81 52 757 6799; Tel: +81 52 757 6771

† Electronic supplementary information (ESI) available. See DOI: 10.1039/c5ra13885j

became complex, and there is a need to develop a precise process taking into account the potential interaction of nanocarriers with pathogenic agents. In addition, understanding their activity is important for the formulation of suitable nanocarriers. In our previous studies, we used the field emission electron microscopy (FE-SEM) with hydrophilic ionic liquid (IL) to observe the fine morphology of the biofilm, including bacterial cells.[22] IL enables to observe fine morphology of wet materials by using simple method. The protein structure of *Staphylococcus epidermidis* bacterial cell fibrils was also revealed by transmission electron microscopy (TEM) with IL. Some researchers have reported that the fine morphology of biological appendages was difficult to observe using a conventional method.[23,24] Therefore, we focused on electron microscopic observation using an optimized method with IL. In 1991, Wilkes *et al.* have reported that ILs consist of cations and anions and, can exist in a fluid state at room temperature (RT).[25] Due to its advantageous properties, such as negligible vapor pressure, high conductivity, and nonflammability, some reports have recently revealed the possibility of a simple observation method for biological materials using an electron microscope.[26–28] IL can protect the morphology of biological materials and prevent charging of sample in EM due to its high conductive property. Our previous studies also showed that some wet materials, including agar gel, hydrous hydroxyapatite green body, hydrous montmorillonite, and swelled seaweed, can be observed using an optimized method by FE-SEM and TEM.[29–32]

In the present study, we tried to establish a preparation method of nanopolymeric micelles based on Soluplus® to cure of biofilm infection disease. We describe the antibacterial activities against the biofilm of four types of polymeric nanocarriers prepared using PLGA and Soluplus®. The micromorphological observation of the antibacterial activity was performed by FE-SEM using optimized sample preparation with hydrophilic IL. In addition, quantitative analyses of antibacterial activity derived from nanocarriers have been carried out.

Methods

Materials

The bacterial strain used for the biofilm formation was *S. epidermidis* (ATCC 14990). This strain was stored at −80 °C and routinely grown at 37 °C for 24 h in 0.5% CO_2 in tryptone soy broth supplemented with 0.25% glucose (TSB, Becton, Dickinson and Company Co., USA). Subsequently, the absorbance of the *S. epidermidis* medium was adjusted to 0.2 (for formation of the biofilm) using a UV/visible spectrophotometer at an optical density of 520 nm (OD520, Ultrospec 2100 Pro, GE Healthcare Life Sciences Co., UK). *S. epidermidis* was grown in 24-well plates and incubated for 24 h at 37 °C. PLGA (lactide : glycolide = 75 : 25; MW = 20 000) used for an antibacterial nanocarrier was purchased from Wako pure chemical industries Ltd, Japan. Soluplus® was kindly given by BASF Japan Ltd (Fig. S1†). Polyvinyl alcohol (Kuraray Poval® PVA 403, polymerization 300, saponification 78–82 mol%, PVA) was purchased from Kuraray Co., Japan. Hydroxypropyltrimonium chitosan (CS) was obtained from Katakurachikkarin Co., Japan. The hydrophilic IL, 1-butyl-3-methylimidazolium tetrafluoroborate (BMIM)(BF4), used for the FE-SEM observation was purchased from Kanto Chemical Co., Japan and dried in a vacuum desiccator at 60 °C for 1 day. Water content of IL was below 128 ppm.

Preparation of PLGA NPs and Sol micelles by the emulsion solvent diffusion (ESD) method

The unmodified PLGA NPs and PLGA NPs modified with CS were prepared by the ESD method using water, as described elsewhere.[15] The unmodified Soluplus® and Soluplus® micelles modified with CS were prepared as below. 6-Coumarin (10 mg), Sol (950 mg), and sodium lauryl sulfate (50 mg) were dissolved in 4 mL of a mixture of acetone and ethanol (acetone : ethanol = 1 : 1). The resulting organic solution was poured into 25 mL of an aqueous PVA solution (2% w/v in distilled water) and stirred at 400 rpm at RT using a propeller-type agitator with three blades. The obtained solution was dialyzed to achieve a higher concentration and remove the organic solvent (Spectra/Por® Dialysis Membrane Pre-wetted RC tubing, MWCO 2 kD, SPECTRUM® LABORATORIES INC., USA) using a semi-permeable membrane in 35% PVA solution under stirring (25 rpm for 24 h) at RT. The resulting solution was freeze dried. To prepare Sol micelles modified with CS, 6-coumarin (10 mg) was added to a mixture of acetone and ethanol. In addition, CS (0.25% w/v in distilled water) and PVA (2% w/v) were used during the dispersing phase of the ESD process. The detailed methodology is illustrated in Fig. 1. The unmodified PLGA NPs, PLGA NPs modified with CS, unmodified Soluplus® micelles, and Soluplus® micelles modified with CS are abbreviated N-PLGA, CS-PLGA, N-Sol and CS-Sol, respectively.

Analysis of the physicochemical properties of PLGA NPs and Sol micelles

The particle size and zeta potential of N-PLGA, CS-PLGA, N-Sol, and CS-Sol were determined using a Zetasizer Nano ZS90 (Malvern Instruments Ltd, Malvern, UK). The N-PLGA and N-Sol was observed using FE-SEM (JXA-8530FA, JEOL Co., Japan) with an accelerating voltage of 10.0 kV and TEM (JEM2100, JEOL Co., Japan) with an accelerating voltage of 200.0 kV using a cooling holder. The samples for FE-SEM and TEM observations were

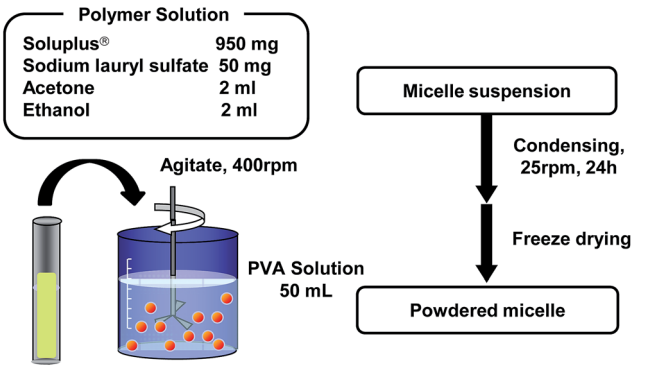

Fig. 1 Schematic procedure for the preparation of Soluplus® micelles.

dispersed in water and skimmed off by a copper mesh with carbon-coated plastic microholes. Subsequently, these samples were coated by platinum sputtering (JUC-5000, JEOL Co., Japan). The sample for TEM observation was cooled from RT to liquid nitrogen temperature at 100 K.

Quantification of nanocarriers adhered to the biofilm

After the biofilm had formed in a 24-well plate, it was washed with purified water and then treated with nanocarrier suspensions (N-PLGA, CS-PLGA, N-Sol, and CS-Sol) at 1 mg mL^{-1} concentrations in TSB medium. After treatment with nanocarriers, plates were incubated for 2 h at 37 °C in 0.5% CO_2. The plates were washed with purified water and scraped using a cell scraper. The phenol–sulfuric acid method was used to quantify the formed biofilm.[33] Each sample (500 μL) was transferred in a test tube with 500 μL of 5 wt% phenol and vortexed. Sulfuric acid (2.5 mL) was rapidly added and tubes were allowed to stand for 30 min at RT. The absorbance of the yellow-orange color was measured with an UV spectrophotometer at 490 nm (U-2800A, HITACHI Co., Japan). To quantify nanocarriers, the 6-coumarin fluorescent dye was extracted from nanocarriers by mixing each sample (750 μL) with chloroform (750 μL) and vortexing for 1 h. Each sample was measured using a fluorophotometer. The excitation/emission wavelengths were 490/520 nm (green). Adhesiveness was expressed as the amount (μg) of nano-carriers associated with each unit weight (μg) of the biofilm glucose.

Determination of minimum inhibitory concentration (MIC) and minimum bactericidal concentration (MBC)

MIC is defined as the lowest concentration of an antimicrobial agent that inhibited the visible growth of microorganism after incubation of 24 h. Four types of nanocarriers (N-PLGA, CS-PLGA, N-Sol, and CS-Sol) were suspended in TSB medium at concentrations of 50, 45, 40, 35, 30, 25, 20, 15, 10, 5, 2.5, 2, 1.5, 1, 0.75, and 0.5 mg mL^{-1} and ultrasonicated. 10 μL of the *S. epidermidis* bacterial cells adjusted to 1.0 using a UV/visible spectrophotometer was added to the each suspension. Subsequently, the suspension was incubated at 37 °C for 24 h in 0.5% CO_2. Bacterial inoculum without any treatment was prepared as a control. Resazurin dye was used to characterize the viability of bacteria. 10 μL of resazurin solution with 0.01% concentration was added to the suspension. The samples were incubated at 37 °C for 2 h and observed. MBC is the lowest concentration of an antibacterial agent required to kill the bacteria. To determine the MBC, each MIC samples were plated in agar plates. Subsequently, these plates were incubated at 37 °C for 24 h and observed. All tests were performed in triplicates.

Antibacterial assay using LIVE/DEAD BacLight bacterial viability kit

Antibacterial assay was performed using LIVE/DEAD BacLight bacterial viability kit (L-13152) (Life Technologies Co., Japan). For a cytotoxicity assay of the biofilm after various treatments, the sample was prepared as follows. After confluent growth of the biofilm in a well, it was washed with purified water then treated with N-PLGA, CS-PLGA, N-Sol, and CS-Sol. The detail method of antibacterial assay using LIVE/DEAD BacLight bacterial viability kit was described elsewhere.[34] The percentage of viable cells after various treatments was calculated.

Confocal laser scanning microscopy observation of the biofilm treated with nanocarriers

The biofilm in a 24-well plate was washed with purified water and exposed to nanocarrier suspensions in TSB medium adjusted to 0.5 and 3.0 mg mL^{-1}. After the treatment with CS-PLGA NPs and CS-Sol micelles used as nanocarriers, the 24-well plate was incubated for 2 h at 37 °C in 0.5% CO_2. The incubated biofilms were washed with purified water and stained using a safranin solution (2% w/v in distilled water) for 2 h. Subsequently, samples were washed with purified water and scraped using a cell scraper. The samples were observed under an LSM 510 META microscope (Carl Zeiss Co., Gottingen, Germany). The excitation/emission wavelengths were 488/535 nm (green) for coumarin (nanocarriers) and 485/625 nm (red) for safranin (biofilm), respectively. CS-PLGA NPs and CS-Sol micelles at 0.5 and 3.0 mg mL^{-1} were abbreviated as CS-$PLGA_{0.5}$ and CS-$PLGA_3$ NPs and CS-$Sol_{0.5}$ and CS-Sol_3 micelles, respectively.

FE-SEM observation of the biofilm treated with nanocarriers

The biofilm in a 24-well plate was treated with four types of nanocarrier suspensions (N-PLGA, CS-PLGA, N-Sol, and CS-Sol) at concentrations of 0.5 and 3.0 mg mL^{-1} in TSB medium. After treatment with nanocarriers, the plate was incubated for 2 h at 37 °C in 0.5% CO_2. The biofilms treated with nanocarriers was observed using FE-SEM with an accelerating voltage of 10.0 kV. The biofilms treated with nanocarriers were incubated with 2 mL of phosphate buffered saline (PBS) solution for 2 h. The biofilm was washed with purified water and treated with the IL solution at an IL : water weight ratio of 1 : 200 for 5 min. The biofilm was then scraped using a cell scraper and skimmed off using a copper mesh with carbon-coated plastic microholes for organic samples for observation under FE-SEM. Subsequently, the sample was coated by platinum sputtering. It should be noted that bacterial cells and biofilm without nanocarrier treatment were not coated by platinum sputtering. The detailed method was described elsewhere.[22]

Results and discussion

Physicochemical properties of nanocarriers

N-PLGA and CS-PLGA, prepared by the ESD method using water, are biodegradable particles. N-Sol and CS-Sol are amphiphilic micelles. The preparation method of Sol is shown in Fig. 1. Table 1 shows the particle size and zeta potential properties of four types of nanocarriers evaluated in this study. The average particle size of N-PLGA, CS-PLGA, N-Sol, and CS-Sol were 251.0 ± 1.9, 357.4 ± 3.4, 50.9 ± 0.8, and 79.5 ± 0.8, respectively. The size of nanocarriers is larger because of the adsorption of CS on the surface. The results obtained with N-PLGA and CS-PLGA were in good agreement with our previous study. N-Sol and CS-Sol micelles were below 100 nm in size. Zeta potentials of N-PLGA, CS-PLGA, N-Sol, and CS-Sol were −18.2 ± 0.7, 17.4 ± 1.2, −17.7

Table 1 Particle size and zeta potential of four kinds of NPs. Data are shown as mean ± SD ($n = 3$)

Condition	N-PLGA	CS-PLGA	N-Sol	CS-Sol
Size (nm)	251.0 ± 1.9	357.4 ± 3.4	50.9 ± 0.8	79.5 ± 0.8
Zeta potential (mV)	−18.2 ± 0.7	17.4 ± 1.2	−17.7 ± 1.1	18.1 ± 1.1

± 1.1, and 18.1 ± 1.1 mV, respectively. N-PLGA had a negative zeta potential due to the dissociation of the carboxyl group of PLGA in distilled water. N-Sol also had a negative zeta potential because we used sodium lauryl sulfate to prepare Sol. CS-PLGA and CS-Sol had a highly-positive zeta potential due to the protonation of the amino group of CS. Fig. 2 shows schematic and FE-SEM and TEM images of N-PLGA and N-Sol. As shown in Fig. 2a, N-PLGA exists as a polymeric matrix structure,[13] while N-Sol micelles exhibit a micelle structure (Fig. 2b). Sanada *et al.* have reported the inner structure of polymeric micelles using small-angle X-ray scattering.[35] The N-Sol polymeric micelle consists of a hydrophobic core and a hydrophilic shell. The FE-SEM images show the morphology of N-PLGA NPs and N-Sol micelles. N-PLGA of around 250 nm has a spherical shape (Fig. 2c). N-Sol micelles of a size below 100 nm are also spherical shape (Fig. 2e). The TEM images show the structure of N-PLGA NPs and N-Sol micelles (Fig. 2d and f). The TEM images revealed that dense of N-PLGA was high compared to that of N-Sol. The sizes of N-PLGA and N-Sol taken by the FE-SEM and TEM were similar to sizes measured with the dynamic light scattering method (Table 1). These results indicate that Sol micelles were successfully prepared using the new method shown in Fig. 1.

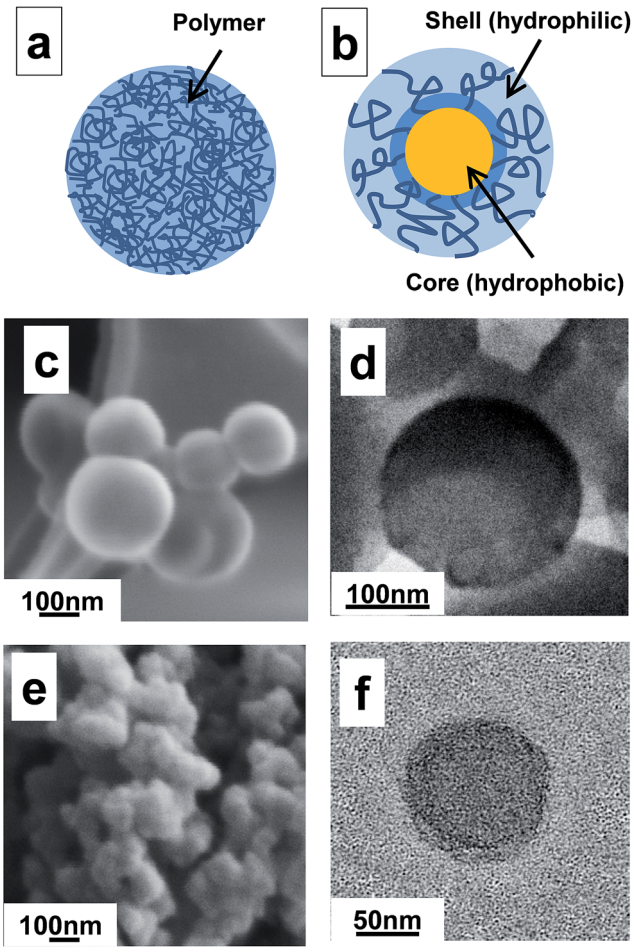

Fig. 2 Schematic description of N-PLGA (a) and N-Sol (b). FE-SEM and TEM images of N-PLGA (c and d) and N-Sol (e and f). N-PLGA exists as polymeric matrix structure. N-Sol consists of a hydrophobic core and a hydrophilic shell.

Quantification of nanocarriers adhered to the biofilm

Fig. 3 shows the amount of nano-carriers adhered to the biofilm based on the spectrophotometric measurement of the biofilm and the fluorometric measurement of nanocarriers. Each nanocarrier was fluorescently labelled with 6-coumarin. Previous studies indicated that polymeric NPs can be labeled uniformly using 6-coumarin and are stable under neutral (pH 7.4) and acidic (pH 5.0) conditions without any release of 6-coumarin.[36] The amount of nanocarriers in the biofilm was estimated from the fluorescence intensity of 6-coumarin extracted from the biofilm lysate sample. In the case of N-PLGA, the amount of adhered NPs to the biofilm was quite small during the 2 h incubation at 37 °C. By CS modification of PLGA NPs, double amount of NPs was adhered to the biofilm. In the case of N-Sol, a large amount of adhered micelles were observed regardless of the CS modification. The surface modification with CS increased the amount of micelles adhered to the biofilm. These results show that Sol micelles have a higher adherence than PLGA NPs. Sol micelles and PLGA NPs adhere to the biofilm *via* different mechanism. While the charge of the NP surface is important for PLGA NPs to adhere to the biofilm, Sol micelles can adhere independently of their charge.

Antibacterial studies using MIC and MBC

The MIC and MBC values of the four types of nanocarriers are listed in Table 2. The MIC values of N-PLGA, CS-PLGA, N-Sol, and CS-Sol were 50, 25, 2.5, 1 mg mL^{-1}, respectively, while the MBC values of N-PLGA, CS-PLGA, N-Sol, and CS-Sol were 50, 30, 5, 2 mg mL^{-1}, respectively. CS-Sol has the lowest MIC and MBC for the *S. epidermidis* bacterial cells. On the other hand, the MIC and MBC values of N-PLGA was drastically high. It showed the lowest antimicrobial ability. It should be noted that the MBC value of each nanocarriers reflect the MIC value.

Antibacterial assay using LIVE/DEAD BacLight bacterial viability kit

Fig. 4 shows the percentage of viable bacteria derived from the biofilms after each of various treatments. The percentages of

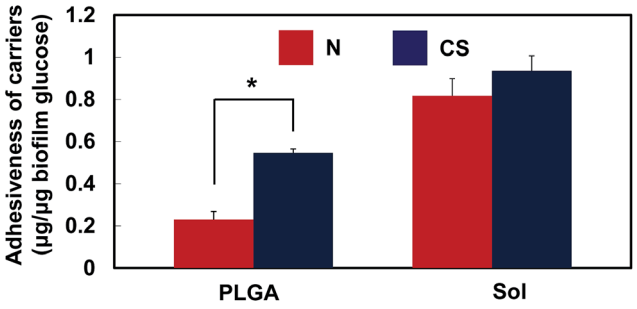

Fig. 3 Adhesiveness of four types of nanocarriers against the biofilm. The concentration of each nanocarriers was 1.0 mg mL^{-1}. Data are shown as mean ± SD ($n = 3$). *$p < 0.05$. N (red) and CS (blue) indicates unmodified and modified with CS, respectively.

Table 2 MIC and MBC values of N-PLGA, CS-PLGA, N-Sol, and CS-Sol ($n = 3$)

	MIC (mg mL^{-1})	MBC (mg mL^{-1})
N-PLGA	50	50
CS-PLGA	25	30
N-Sol	2.5	5
CS-Sol	1	2

viable bacteria after treatment with N-PLGA, CS-PLGA, N-Sol, and CS-Sol were 84.2, 63.4, 47.0, and 31.0%, respectively. Only 15.8% of bacterial cells died following N-PLGA treatment. Similar to previous study, the percentage of viable bacteria was drastically decreased by CS modification. On the other hand, 53.0% of bacterial cells died following N-Sol treatment although no CS modification. The antibacterial activity of Sol was increased 16.0% by the CS modification. From these results, CS-Sol had the highest antibacterial activity among the four formulations.

Confocal imaging of various nanocarriers in the biofilm

The penetration behaviour of CS-PLGA and CS-Sol was visualized by confocal laser scanning microscopy. For comparison, the biofilm without any treatment was observed as a control. Fig. 5a shows the confocal fluorescence image of the biofilm stained by safranin, and the biofilm was observed in intact configuration. No nanocarriers were detected (Fig. 5b). Confocal fluorescence images of the safranin-stained biofilm treated with 6-coumarin labeled nanocarriers are shown in Fig. 5c–j. Fig. 5c–f shows the biofilm treated with CS-PLGA. The biofilm surface was partially eroded by CS-$PLGA_{0.5}$ (Fig. 5c), and some CS-PLGA could be detected, particularly at the surface of the biofilm where NPs had adhered (Fig. 5d). In the case of CS-$PLGA_3$, a thick film of the biofilm was eroded, and bacterial cells inside the biofilm could be observed (Fig. 5e). A thick film of EPS covers the surface of bacteria to construct a 3D mature structure.[9] CS-PLGA can remove EPS by exerting an antibacterial effect. Planktonic cells appeared around the biofilm after erosion of the thick film of the biofilm (indicated by black arrow). CS-PLGA was observed on the surface and the inner part of the biofilm (Fig. 5f).

Fig. 5g–j shows the biofilm treated with CS-Sol. In the case of CS-$Sol_{0.5}$, the thick film covering the surface of bacterial cells was eroded and the aggregation of bacterial cells was observed in the inner part of the biofilm (Fig. 5g). There were many voids on the surface of the eroded biofilm. Some parts of bacterial cells were removed by CS-Sol and existed as pores (indicated by black arrows). CS-Sol was observed on the surface and in the inner part of the aggregation of bacterial cells (Fig. 5h). In the case of CS-Sol_3, erosion of the thick film was preceded compared to CS-$Sol_{0.5}$ treatment (Fig. 5i). It can be seen many planktonic cells exist around the aggregation of bacterial cells (indicated by black arrows). The Sol micelles were difficult to observe because of their small size (Fig. 5j). Fig. S2† shows confocal fluorescence images of CS-Sol adhered to the biofilm at a high magnification. The erosion of the biofilm was lower with CS-PLGA than that with CS-Sol. With CS-Sol, the thick film covering the surface of bacterial cells was almost eroded. In parallel, some bacterial colonies were separated and only small-sized bacterial cell aggregations were observed. However, the fine morphology of nanocarriers and bacterial cells was not observed by confocal laser scanning microscopy. Thus, we examined the antibacterial activity against the biofilm of nanocarriers with FE-SEM.

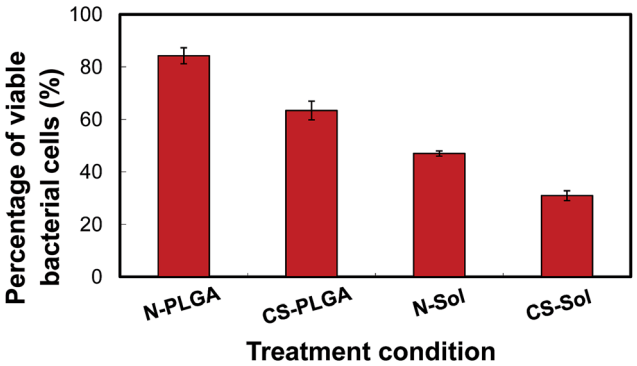

Fig. 4 Percentage of viable bacterial cells after various treatments. Data are shown as mean ± SD ($n = 3$).

The antibacterial activity of N-PLGA, CS-PLGA, N-Sol, and CS-Sol against the biofilm observed by FE-SEM

In the present study, the antibacterial activities of four types of nanocarriers (N-PLGA, CS-PLGA, N-Sol, and CS-Sol) were observed using FE-SEM with hydrophilic IL. Fig. 6 shows the morphology of *S. epidermidis* bacterial cells cultivated during 6 h and the biofilm formed in 24 h in the absence of nanocarriers by FE-SEM. As shown in Fig. 6a, small colonies were formed by bacterial cells cultivated during 6 h. The spherical shape of the bacterial cell measures approximately 1 μm. After 24 h cultivation, a bacterial agglomerate covered by a thick EPS film was observed and no individual bacterial cell could be observed (Fig. 6b). At a high magnification, the thick film covering the surface of bacterial cells was clearly observed

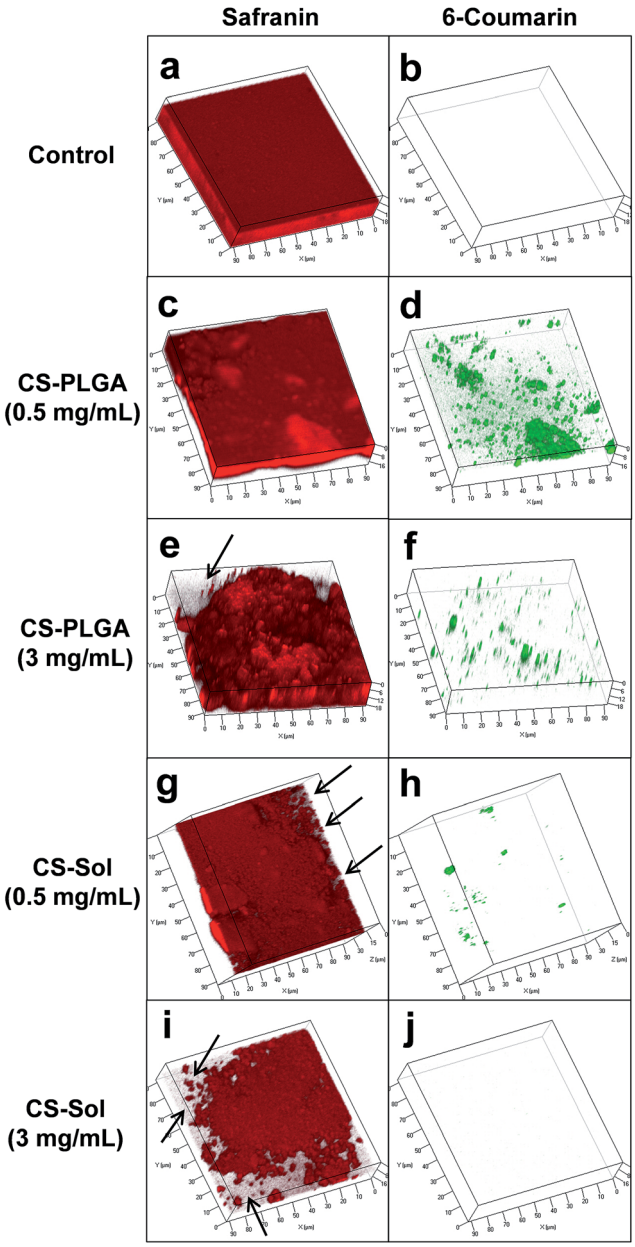

Fig. 5 Confocal laser microscopy images of the biofilm without any treatment (a) (b), treated with coumarin (green)-labelled CS-PLGA$_{0.5}$ (c and d), CS-PLGA$_3$ (e and f), CS-Sol$_{0.5}$ (g and h), and CS-Sol$_3$ (i and j). Biofilm was stained with safranin (red). For each condition, two fluorescence images (excitation at 488 nm and emission at 535 nm for the 6-coumarin; excitation at 485 nm and emission at 625 nm for the safranin) were acquired.

(Fig. 6c). There were some holes (˂500 nm in size) on the surface of biofilm similar to our previous study.[22] These holes, named water channels, allow the diffusion of nutrients and oxygen in the biofilm agglomerate. After visualizing, the fine morphology of the target agent, *i.e.*, the biofilm, we aimed to visualize the antibacterial activity of nanocarriers using FE-SEM observation in the next section.

Fig. 7 shows the FE-SEM images of the biofilm treated with N-PLGA for 2 h. The biofilm was treated with two different concentrations of N-PLGA: N-PLGA$_{0.5}$ and N-PLGA$_3$. There was no N-PLGA around the biofilm (Fig. 7a and c). The high magnification images (Fig. 7b and d) show the rough morphology of the thick film derived from the biofilm. N-PLGA seems to have difficulties to adhere to the biofilm surface due to the negative zeta potential (Table 1). These results showed that N-PLGA is not effective for the biofilm removal. Hence, it was found that the surface of the thick EPS film was only slightly eroded by the antibacterial activity of N-PLGA. These results are in good agreement with the quantitative analysis (Fig. 3 and 4). There was no marked difference depending on the amount of N-PLGA because N-PLGA possesses no antibacterial ability.

Fig. 8 shows FE-SEM images of the biofilm treated with CS-PLGA$_{0.5}$ and CS-PLGA$_3$. From low magnification images, it was found that the thick film covering the surface of bacterial cells was eroded by CS-PLGA$_{0.5}$ and CS-PLGA$_3$ NPs (Fig. 8a and c). The bacterial cells were clearly observed because of the thick film removal. Many pores were observed at the biofilm surface with the CS-PLGA$_3$ treatment (Fig. 8c). At a high magnification, CS-PLGA adhering to bacterial cells was clearly observed (Fig. 8b). The particle size observed in the FE-SEM image was similar to that measured with dynamic light scattering (357 nm). The size of the individual bacterial cell was also similar to that of bacterial cells without any treatment (Fig. 6). EPS covering bacterial cells (indicated by an arrow) was clearly observed. In our previous studies, a similar morphology of the biofilm was obtained after 16 h of cultivation.[22] These results indicate that CS-PLGA eroded the thick film of the biofilm by reversing the biofilm formation process. CS-PLGA penetrated into the aggregation of bacterial cells exerting the antibacterial activity after the thick film removal. CS-PLGA NPs with a positive charge can effectively erode the thick film and affect bacterial cells in the biofilm, although N-PLGA NPs have no antibacterial activity. It has been reported that positively charged CS can easily attach to negatively-charged microbial cell membranes *via* electrostatic forces.[37] Raafat *et al.* have

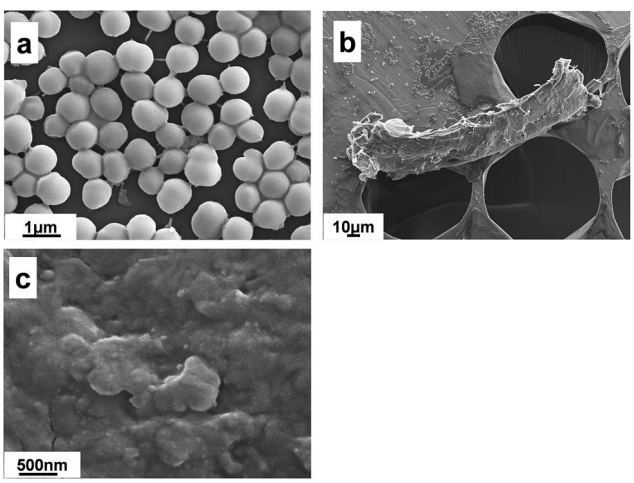

Fig. 6 FE-SEM images of (a) *S. epidermidis* bacterial cells and (b) (c) biofilm without any nanocarriers following pretreatment using the new method with IL. Bacterial cells for these samples were formed in 24-well plates by 6 h and 24 h incubation, respectively.

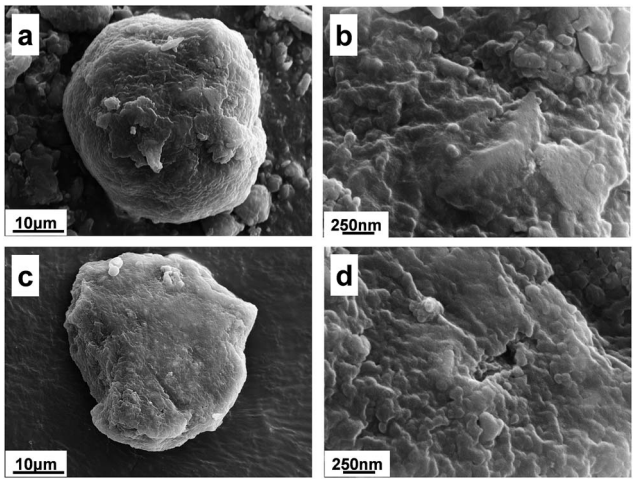

Fig. 7 FE-SEM images of biofilm treated with (a and b) N-PLGA$_{0.5}$, (c and d) N-PLGA$_3$ for 2 h following pretreatment using the new method.

directly observed CS molecules attached to the bacterial cell by TEM.[38] Goy *et al.* have reported that CS could inhibit microorganism growth and multiplication.[39] Additionally, recent studies have proposed an antibacterial mechanism derived from CS.[39] Dutta *et al.* have reported that CS is effective against Gram-positive bacteria, including *S. aureus*.[40] These reports support the quantitative and visualization analyses in the present study. As we used the *S. epidermidis* strain for the biofilm formation, CS in CS-PLGA might work effectively to inhibit the biofilm formation and survival of bacterial cells.

Fig. 9 shows FE-SEM images of the biofilm treated with N-Sol. The biofilm was treated with N-Sol$_{0.5}$ and N-Sol$_3$. From low magnification images, an aggregation formed by bacterial cells was observed by erosion of the thick film of the biofilm (Fig. 9a and c). We could not find the bacterial agglomeration seen in Fig. 6b. The thick film covering the surface of bacteria was totally eroded by N-Sol. There were many voids in the bacterial aggregation. From high magnification images, bacterial cells changed from a spherical to a wrinkled shape after the N-Sol$_{0.5}$ treatment (Fig. 9b), and this was not observed after N-PLGA or CS-PLGA treatment. Moreover, the antibacterial activity of micelles was observed particularly between combined bacterial cells (indicated by yellow arrows in Fig. 9b). In the case of N-Sol$_3$, rod-like structures were observed after erosion of the thick film of the biofilm (indicated by blue arrows in Fig. 9d). Some researchers have reported these type of tubes.[41,42] These rod-like structures have been associated with cytoskeletal and motor proteins playing a role in active transport.[41] Primarily polysaccharide materials fill the void between bacterial cells during the biofilm formation. Therefore, polysaccharide materials were likely eroded by N-Sol. From the dynamic light scattering measurement, the size of N-Sol was found to be 50 nm, which was slightly smaller than the size observed in the FE-SEM and TEM image. The difference is explained by the maintenance of the Sol structure in the liquid condition as Sol was treated with liquid IL for the sample preparation. The size of the bacterial cell obtained in Fig. 9 is different from the untreated bacterial cell. Depending on the amount of N-Sol, the bacterial cell size was decreased, a phenomenon not observed in the case of PLGA. It was found that N-Sol promotes the removal of EPS around bacterial cells and the shrinkage of bacterial cells. Some researchers have reported that the surfactant has a biocide effect on bacterial cells.[43,44] Induction of cell autolysis and inhibition of respiration by surfactants have also been reported.[45] According to these reports, bacterial cells were damaged by Sol micelles. Moreover, Kramer *et al.* have suggested that sodium lauryl sulfate attacks the cell membrane *via* membrane proteins.[46] In the present study, we have used sodium lauryl sulfate for the preparation of Sol micelles. Hence, bacterial cells might have been affected by Sol micelle treatment. In addition, we have revealed that Sol tend to adhere to hydrophobic materials compared to PLGA NPs due to Sol is amphiphilic material (data not shown). It is explained that N-Sol have high adhesive property to the biofilm even under hydrophobic

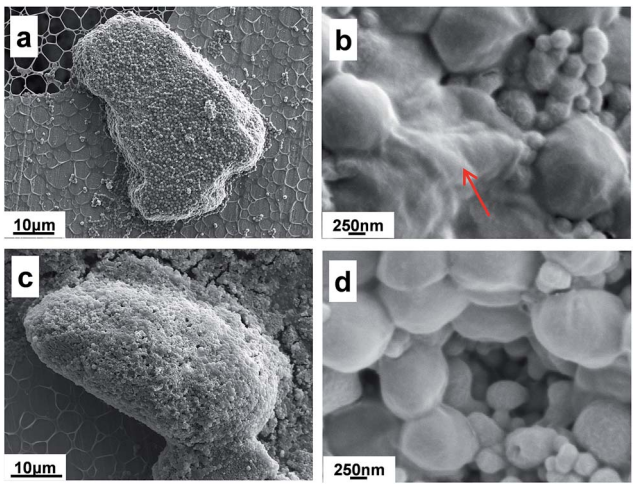

Fig. 8 FE-SEM images of biofilm treated with (a and b) CS-PLGA$_{0.5}$, (c and d) CS-PLGA$_3$ for 2 h following pretreatment using the new method.

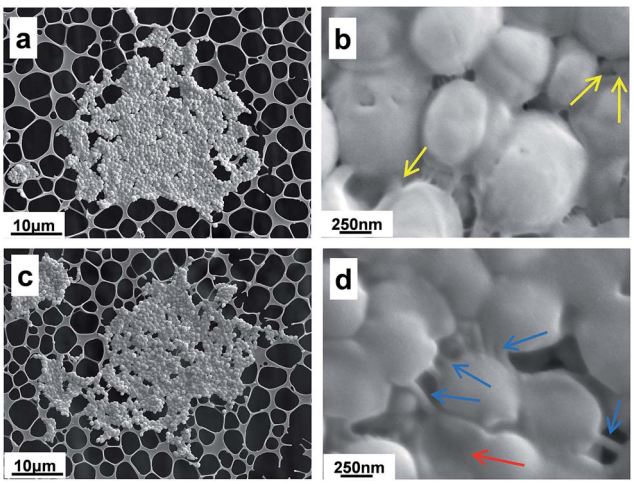

Fig. 9 FE-SEM images of biofilm treated with (a and b) Sol$_{0.5}$, (c and d) Sol$_3$ for 2 h following pretreatment using the new method.

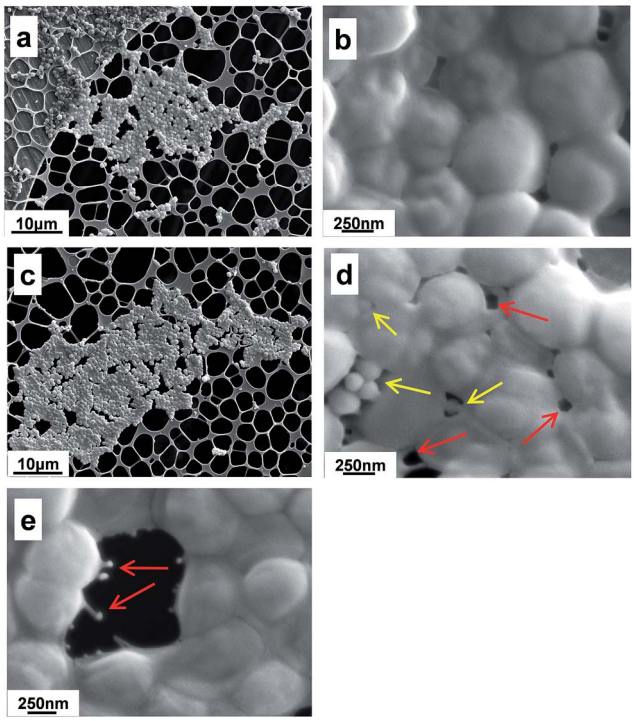

Fig. 10 FE-SEM images of biofilm treated with (a) (b) CS-$Sol_{0.5}$, (c)–(e) CS-Sol_3 following pretreatment using the new method.

condition. These facts might be proceeded high adhesiveness, erosion and antibacterial activities against both the biofilm and bacterial cells, although N-Sol has a negative zeta potential. N-Sol seems to exert antibacterial activity because of high adhesive property to hydrophobic part within bacterial cell.

Fig. 10 shows FE-SEM images of the biofilm treated with CS-Sol using FE-SEM with IL. The biofilm was treated with CS-$Sol_{0.5}$ and CS-Sol_3. Similar to the case of N-Sol, a bacterial agglomeration with a 3D structure was not observed (Fig. 10a and c). The volume of aggregation formed by bacterial cells was slightly low. At a high magnification, wrinkled and flat shaped bacterial cells were observed (Fig. 10b and d). CS-Sol adhered between combined bacterial cells and penetrated into bacterial cells with the antibacterial activity (indicated by yellow arrows in Fig. 10d). The size of CS-Sol was a little bigger than that measured with dynamic light scattering. These facts are in agreement with N-Sol (Fig. 9d). In the case of CS-Sol_3, many pores derived from the antibacterial activity of CS-Sol were observed (indicated by red arrows in Fig. 10d). Fig. 10e shows some fibrils attacked by CS-Sol. The shape of the edge of fibrils changed from straight to round. In general, the fibril of *S. epidermidis* bacterial cell extends straight from one cell to another without branching. The fibril was reported to have an important role in the biofilm formation process.[47,48] As indicated by red arrows in Fig. 10e, the fibril was directly attacked and inhibited the biofilm formation. This shows that CS-Sol micelles have a specific antibacterial activity directed towards the fibril.

The antibacterial activity of four types of polymeric nanocarriers against the biofilm was successfully observed using this IL treatment and an optimized observation method. These results clearly demonstrate that PLGA and Sol have different antibacterial activities against the biofilm.

Conclusions

We have successfully developed preparation method for nanocarriers of polymeric micelles based on Sol. To design effective carriers with high antibacterial activities, four types of polymeric nanocarriers were compared. In the present study, the antibacterial activity derived from each N-PLGA, CS-PLGA, N-Sol, and CS-Sol on the biofilm formed by *S. epidermidis* bacterial cells was characterized by a combination of quantitative and visualization analyses. Using a new observation methodology with hydrophilic IL, the microscopic evaluation of the antibacterial activity was established. These results show different antibacterial activities of polymeric nanocarriers on the biofilm. Sol micelles have a high antibacterial activity regardless of CS modification on the surface of micelles. PLGA NPs exerted an antibacterial effect by CS modification. CS-Sol showed the highest antibacterial activity against the biofilm among the four tested nanocarriers. CS-Sol was found to directly attack the fibril, which works for the bacterial multiplication and biofilm formation. Obtaining these detailed activities of polymeric nanocarriers is difficult with conventional methods. The optimized observation method can be used to reveal the antibacterial activity of polymeric nanocarriers to target pathogenic agents. Moreover, the developed novel Sol micelles can contribute as effective nanocarriers for antibacterial DDS in the treatment of biofilm infections.

Acknowledgements

This study was partially supported by JSPS KAKENHI Grant Number 25460046, 50574448 and the research Grant from the Institute of Pharmaceutical Life Sciences, Aichi Gakuin University.

Notes and references

1 A. M. Gutierrez-Colina, C. Eaton, P. Cheng, M. Strieper, P. Frias, K. Gooden and R. L. Blount, *J. Dev. Behav. Pediatr.*, 2014, **35**, 360–366.
2 Y. M. Chen, A. P. Dai, Y. Shi, Z. J. Liu, M. F. Gong and X. B. Yin, *Int. J. Infect. Dis.*, 2014, **29**, 279–286.
3 S. Veerachamy, T. Yarlagadda, G. Manivasagam and P. K. Yarlagadda, *Proc. Inst. Mech. Eng., Part H*, 2014, **228**, 1083–1099.
4 K. L. Rogers, P. D. Fey and M. E. Rupp, *Infect. Dis. Clin.*, 2009, **23**, 73–98.
5 R. O. Darouiche, *Clin. Infect. Dis.*, 2001, **33**, 1567–1572.
6 L. G. Harris and R. G. Richards, *Injury*, 2006, **37**(suppl. 2), S3–S14.
7 C. N. Murphy and S. Clegg, *Future Microbiol.*, 2012, **7**, 991–1002.
8 G. N. Belibasakis, G. Charalampakis, N. Bostanci and B. Stadlinger, *Adv. Exp. Med. Biol.*, 2015, **830**, 69–84.

9 R. M. Donlan, *Emerging Infect. Dis.*, 2002, **7**, 277–281.
10 J. W. Costerton, Z. Lewandowski, D. E. Caldwell, D. R. Korber and H. M. Lappin-Scott, *Annu. Rev. Microbiol.*, 1995, **49**, 711–745.
11 L. Li, Z. Bai and P. A. Levkin, *Biomaterials*, 2013, **34**, 8504–8510.
12 V. Karavelidis, D. Bikiaris and K. Avgoustakis, *J. Pharm. Pharmacol.*, 2015, **67**, 215–230.
13 Y. Kawashima, H. Yamamoto, H. Takeuchi, T. Hino and T. Niwa, *Eur. J. Pharm. Biopharm.*, 1998, **45**, 41–48.
14 H. Yamamoto, Y. Kuno, S. Sugimoto, H. Takeuchi and Y. Kawashima, *J. Controlled Release*, 2005, **2**, 373–381.
15 K. Tahara, T. Sakai, H. Yamamoto, H. Takeuchi and Y. Kawashima, *Int. J. Pharm.*, 2008, **354**, 210–216.
16 H. Yamamoto, K. Tahara and Y. Kawashima, *J. Microencapsulation*, 2012, **29**, 54–62.
17 K. Tahara, S. Tadokoro, H. Yamamoto, Y. Kawashima and N. Hirashima, *Biomaterials*, 2012, **33**, 343–351.
18 M. Yang, H. Yamamoto, H. Kurashima, H. Takeuchi, T. Yokoyama, H. Tsujimoto and Y. Kawashima, *Eur. J. Pharm. Sci.*, 2012, **30**, 235–243.
19 R. N. Shamma and M. Basha, *Powder Technol.*, 2013, **237**, 406–414.
20 T. Obata, Y. Suzuki, N. Ogawa, I. Kurimoto, H. Yamamoto, T. Furuno, T. Sasaki and M. Tanaka, *Biol. Pharm. Bull.*, 2014, **37**, 802–807.
21 R. Shamma and N. Elkasabgy, *Drug Delivery*, 2014, **3**, 1–11.
22 C. Takahashi, G. Kalita, N. Ogawa, K. Moriguchi, M. Tanemura, Y. Kawashima and H. Yamamoto, *Anal. Bioanal. Chem.*, 2015, **407**, 1607–1613.
23 Y. Ishigaki, Y. Nakamura, T. Takehara, N. Nemoto, T. Kurihara, H. Koga, T. Takegami, H. Nakagawa, N. Nemoto, N. Tomosugi, S. Kuwabata and S. Miyazawa, *Microsc. Res. Tech.*, 2011, **74**, 415–420.
24 K. Yanaga, N. Maekawa, N. Shimomura, Y. Ishigaki, Y. Nakamura, T. Takegami, N. Tomosugi, S. Miyazawa and S. Kuwabata, *Mycol. Progr.*, 2012, **11**, 343–347.
25 J. S. Wilkes and M. J. Zaworotko, *J. Chem. Soc., Chem. Commun.*, 1992, 965–967.
26 S. Kuwabata, T. Tsuda and T. Torimoto, *J. Phys. Chem. Lett.*, 2010, **1**, 3177–3188.
27 T. Tsuda, N. Nemoto, K. Kawakami, E. Mochizuki, S. Kishida, T. Tajiri, T. Kushibiki and S. Kuwabata, *ChemBioChem*, 2010, **12**, 2547–2550.
28 A. Dwiranti, L. Lin, E. Mochizuki, S. Kuwabata, A. Takaoka, S. Uchiyama and K. Fukui, *Microsc. Res. Tech.*, 2012, **75**, 1113–1118.
29 C. Takahashi, T. Shirai and M. Fuji, *Mater. Chem. Phys.*, 2012, **133**, 565–572.
30 C. Takahashi, T. Shirai and M. Fuji, *Microsc. Res. Tech.*, 2013, **76**, 66–71.
31 C. Takahashi, D. K. Pattanayak, T. Shirai and M. Fuji, *J. Eur. Ceram. Soc.*, 2013, **33**, 629–635.
32 C. Takahashi, D. K. Pattanayak, T. Shirai and M. Fuji, *RSC Adv.*, 2014, **4**, 27322–27328.
33 M. Dubois, K. A. Gilles, J. K. Hamilton, P. A. Rebers and F. Smith, *Anal. Chem.*, 1956, **28**, 350–356.
34 C. Takahashi, N. Ogawa, Y. Kawashima and H. Yamamoto, *Microscopy*, 2015, **64**, 169–180.
35 Y. Sanada, I. Akiba, K. Sakurai, K. Shiraishi, M. Yokoyama, E. Mylonas, N. Ohta, N. Yagi, Y. Shinohara and Y. Amemiya, *J. Am. Chem. Soc.*, 2013, **135**, 2574–2582.
36 K. Tahara, Y. Kato, H. Yamamoto, J. Kreuter and Y. Kawashima, *J. Microencapsulation*, 2011, **28**, 29e36.
37 G. J. Tsai and W. H. Su, *J. Food Prot.*, 1999, **62**, 239–243.
38 D. Raafat, K. von Bargen, A. Haas and H. G. Sahl, *Appl. Environ. Microbiol.*, 2008, **74**, 3764–3773.
39 C. G. Rejane, B. Douglas and B. G. A. Odilio, *Polim.: Cienc. Tecnol.*, 2009, **19**, 241–247.
40 P. K. Duttaa, S. Tripathia, G. K. Mehrotraa and J. Duttab, *Food Chem.*, 2009, **114**, 1173–1182.
41 D. M. Davis and S. Sowinski, *Nat. Rev. Mol. Cell Biol.*, 2008, **9**, 431–436.
42 G. P. Dubey and S. Ben-Yehuda, *Cell*, 2011, **144**, 590–600.
43 D. J. Hess, M. J. Henry-Stanley and C. L. Wells, *Antimicrob. Agents Chemother.*, 2014, **58**, 6970–6973.
44 I. M. Banat, M. A. de Rienzo and G. A. Quinn, *Appl. Microbiol. Biotechnol.*, 2014, **98**, 9915–9929.
45 T. Tsuchido, A. Svarachorn, H. Soga and M. Takano, *Antimicrob. Agents Chemother.*, 1990, **34**, 781–785.
46 V. C. Kramer, D. M. Calabrese and K. W. Nickerson, *Appl. Environ. Microbiol.*, 1980, **40**, 973–976.
47 M. A. Banner, J. G. Cunniffe, R. L. Macintosh, T. J. Foster, H. Rohde, D. Mack, E. Hoyes, J. Derrick, M. Upton and P. S. Handley, *J. Bacteriol.*, 2007, **189**, 2793–2804.
48 R. L. Macintosh, J. L. Brittan, R. Bhattacharya, H. F. Jenkinson, J. Derrick, M. Upton and P. S. Handley, *J. Bacteriol.*, 2009, **191**, 7007–7016.